Development 103, 675–686 (1988)
Printed in Great Britain © The Company of Biologists Limited 1988

Behaviour of microtubules and actin filaments in living *Drosophila* embryos

DOUGLAS R. KELLOGG, TIM J. MITCHISON and BRUCE M. ALBERTS

Department of Biochemistry and Biophysics, University of California, San Francisco, California 94143-0448, USA

Summary

We describe the preparation of novel fluorescent derivatives of rabbit muscle actin and bovine tubulin, and the use of these derivatives to study the behaviour of actin filaments and microtubules in living *Drosophila* embryos, in which the nuclei divide at intervals of 8 to 21 min. The fluorescently labelled proteins appear to function normally *in vitro* and *in vivo*, and they allow continuous observation of the cytoskeleton in living embryos without perturbing development. By coinjecting labelled actin and tubulin into the early syncytial embryo, the spatial relationships between the distinct filament networks that they form can be followed second by second. The dynamic rearrangements of actin filaments and microtubules observed confirms and extends results obtained from previous studies, in which fixation techniques and specific staining were used to visualize the cytoskeleton in the *Drosophila* embryo. However, no tested fixation method produces an exact representation of the *in vivo* microtubule distribution.

Key words: microtubule, actin filament, *Drosophila*, cytoskeleton, fluorescence.

Introduction

The early events in *Drosophila* embryogenesis have been extensively studied (Rabinowitz, 1941; Sonnenblick, 1950; Turner & Mahowald, 1976; Zalokar & Erk, 1976; Foe & Alberts, 1983). The first thirteen nuclear divisions occur rapidly in a syncytial cytoplasm. All of the nuclei are initially located in the interior of the embryo, but during nuclear cycles 8 and 9 most nuclei migrate to the cortex of the embryo. By interphase of nuclear cycle 10, these nuclei form a continuous monolayer just beneath the surface of the plasma membrane. The surface nuclei in this 'syncytial blastoderm' embryo divide four more times in a nearly synchronous fashion and then become synchronously cellularized during interphase of nuclear cycle 14; subsequent local infoldings of the newly formed cell sheet mark the beginning of gastrulation.

A number of recent studies suggest that the cytoskeleton plays an important role in the localization of developmental information in early embryos (Edgar *et al.* 1988; Strome & Wood, 1983; Ubbels *et al.* 1983). One therefore suspects that a detailed knowledge of cytoskeletal organization and function will be integral to our understanding of the pattern formation process during embryogenesis. Several recent studies have initiated a characterization of the cytoskeleton in early *Drosophila* embryos (Warn *et al.* 1984, 1985, 1987; Walter & Alberts, 1984; Karr & Alberts, 1986; Warn & Warn, 1986). These studies reveal that two regions of the early embryo have a high density of cytoskeletal filaments. These same regions can be detected in the light microscope as cleared zones that exclude yolk particles and other large organelles (Scriba, 1964). One such region is the cortical layer of cytoplasm that lies just beneath the plasma membrane before the nuclei migrate to the periphery of the embryo. Actin filaments, microtubules and intermediate filaments form a dense meshwork in this cortical cytoplasm to a depth of about 3 μm. The other region that is enriched in cytoskeletal elements constitutes a special 'cytoplasmic domain' that surrounds each nucleus. During interphase in the syncytial blastoderm, microtubules are organized around each nucleus by a pair of centrosomes located on the apical side of the nucleus and actin filaments form a cap-like layer above these centrosomes, just beneath the plasma membrane. By the time that mitosis begins, the centrosomes have

migrated to either side of the nucleus, where they assemble a mitotic spindle. The actin cap enlarges as the nuclear cycle progresses, spreading into transient furrows surrounding each spindle during mitosis and dividing into two smaller caps at telophase. The cytoskeletal rearrangements that take place in the syncytial embryo are remarkable in their rapidity, since the successive nuclear cycles require only 8 (cycle 10) to 21 (cycle 13) min to complete (Foe & Alberts, 1983).

Earlier studies have employed a variety of fixation and staining techniques to visualize the cytoskeleton of the early *Drosophila* embryo. These methods have several disadvantages. One can never be sure that a fixation procedure accurately preserves the *in vivo* distribution of a protein, and the view that one obtains from a fixed specimen is necessarily a static one. In order to circumvent these problems, we have been developing techniques for visualizing fluorescently labelled cytoskeletal proteins that have been injected into living *Drosophila* embryos, similar to the techniques that have been used successfully in other biological systems (for reviews see Taylor & Wang, 1980; Taylor *et al.* 1986). By using novel fluorescent derivatives of actin and tubulin to visualize the behaviour of actin filaments and microtubules during the early syncytial nuclear divisions in the *Drosophila* embryo, the initial studies reported here have allowed us to gain a better understanding of cytoskeletal organization and dynamics in the early *Drosophila* embryo; they have also provided a standard for comparison that has allowed us to develop improved fixation procedures.

Materials and methods

Reagents

5-(4,6-dichlorotriazinyl) amino fluorescein (DTAF), lissamine rhodamine B sulphonyl chloride (LRSC), and *N*-hydroxy succinimidyl 5-carboxytetramethyl rhodamine (NHSR) were obtained from Molecular Probes. Dimethyl formamide and dimethyl sulphoxide were obtained from Aldrich (sure seal grade).

Preparation of fluorescently labelled proteins

Tubulin has been labelled with *N*-hydroxy succinimidyl 5-carboxytetramethyl rhodamine (NHSR) or lissamine rhodamine B sulphonyl chloride (LRSC). For preparation of NHSR-labelled tubulin, 3–4 mg of phosphocellulose purified bovine brain tubulin (Mitchison & Kirschner, 1984) at 1–5 mg ml^{-1} in 80 mM-potassium Pipes (pH 6·8), 1 mM-Na_3EGTA, 1 mM-$MgCl_2$ (buffer designated BRB80) was polymerized into microtubules by adjusting the solution to 10 % dimethylsulphoxide, 1 mM-GTP, and 4 mM-$MgCl_2$, followed by incubation at 37 °C for 25 min. The microtubules were then collected by centrifugation at 35 °C through a 4·5 ml cushion consisting of BRB80 plus 50 % sucrose (60 min at 50 000 revs min^{-1} in a Beckman 50Ti rotor). The pellet was resuspended in enough BRB80 to give a protein concentration of 5–8 mg ml^{-1}, and incubated on ice for 30 min to depolymerize microtubules. The tubulin solution was then clarified for 5 min in a Beckman microfuge and the pellet discarded. This initial cycle of polymerization and depolymerization is necessary to remove the residual β-mercaptoethanol (left over from the tubulin purification procedure) that interferes with the NHSR reaction. The tubulin was repolymerized into microtubules as described above, and then adjusted to 45 % sucrose by addition of prewarmed BRB80 containing 80 % sucrose (the addition of sucrose doubled the subsequent yield). A 50 mg ml^{-1} stock of NHSR was made up in dimethyl formamide and stored at −70 °C. From this stock, NHSR was added to a final concentration of 3 mg ml^{-1} and the reaction was allowed to proceed for 2 h at 37 °C. At the end of the labelling period, the microtubules were collected by centrifugation at 35 °C through a 4·5 ml cushion consisting of BRB80, 50 % sucrose, 10 mM-potassium glutamate, and 5 mM-dithiothreitol (DTT) (60 min at 50 000 revs min^{-1} in a Beckman 50Ti rotor). The pellet was resuspended in 0·4 ml of BRB80 containing 0·1 mM-GTP, 10 mM-potassium glutamate, 5 mM-DTT and incubated on ice for 30 min to depolymerize the microtubules (the potassium glutamate and DTT were included in this step and the preceding one in order to block unreacted NHSR). The tubulin solution was then clarified by centrifugation at 4 °C for 20 min at 50 000 revs min^{-1} (Beckman 50Ti rotor), followed by a brief spin in a microfuge.

In order to remove tubulin damaged by the coupling of rhodamine, the modified tubulin was subjected to two cycles of polymerization and depolymerization. Thus, the supernatant was adjusted to 33 % glycerol, 1 mM-GTP, 4 mM-$MgCl_2$ and the tubulin repolymerized by incubation at 37 °C for 30 min. The microtubules were then pelleted through a 50 % sucrose cushion in BRB80 as previously described. The pellet was resuspended in 0·4 ml of BRB80 containing 0·1 mM-GTP and depolymerized by incubation on ice for 30 min. Insoluble material was removed and the resulting tubulin solution was subjected to an additional round of glycerol-induced assembly and disassembly, in which the microtubule pellet was resuspended in 150 μl of 50 mM-potassium glutamate (pH 6·8), 0·5 mM-$MgCl_2$, before depolymerization on ice for 30 min. This final tubulin solution was then centrifuged at 4 °C for 7 min at 30 lbf in^{-1} (1 lbf in^{-1} ≈ 6·9 kPa) in a Beckman airfuge and the supernatant frozen on liquid nitrogen in small aliquots. The procedure described produces an overall protein yield of 30 % and a stoichiometry that is typically about 0·9 rhodamines per tubulin dimer.

LRSC–tubulin and DTAF–tubulin were prepared in essentially the same manner as NHSR–tubulin, with the following modifications. LRSC was added to the tubulin solution in two equal-sized samples spaced by 5 min. The LRSC was added to a concentration of 0·8 mg ml^{-1} (final) from a 50 mg ml^{-1} stock made up in dimethyl formamide moments before using and the total reaction time was 10 min. Except for terminating the reaction by addition of 10 mM-potassium glutamate, the remainder of the procedure was the same as for NHSR–tubulin and it produced

a stoichiometry of about 1. For DTAF–tubulin, DTAF was added to the reaction in 5 aliquots at 10 min intervals to a final concentration of 2·6 mg ml^{-1}. The DTAF was added from a 50 mg ml^{-1} stock made up in dimethyl formamide and the total reaction time was 2·5 h, producing a stoichiometry of about 0·5.

Drosophila tubulin was prepared by a modification of procedures used by Detrich & Wilson (1983) to purify sea urchin embryo tubulin (D. R. Kellogg, C. M. Field and B. M. Alberts, unpublished data). *Drosophila* tubulin was labelled with LRSC as described for bovine tubulin.

Rabbit muscle actin was prepared according to Pardee & Spudich (1982) and stored at 4°C as filaments at 4–7 mg ml^{-1} in a buffer containing 50 mM-Tris–HCl, pH 8·1, 100 mM-KCl, 0·2 mM-ATP, and 0·02 % sodium azide. For preparation of fluorescently labelled actin, 2–5 mg of this filamentous actin was dialysed for 3 h against 200 ml of 50 mM-potassium Pipes (pH 6·8), 50 mM-KCl, 0·2 mM-$CaCl_2$, and 0·2 mM-ATP. In order to break up actin aggregates, the dialysed actin was stirred vigorously with a Teflon dounce homogenizer (several strokes) and brought to 2–3 mg ml^{-1} by addition of the dialysis buffer. ATP was added to 0·5 mM and NHSR was added to a concentration of 3·2 mg ml^{-1} (from a 50 mg ml^{-1} stock in dimethyl formamide, as described above). The reaction was allowed to proceed for 1 h at room temperature and actin filaments were then pelleted by spinning for 60 min at 50 000 rev min^{-1} in a Beckman 50Ti rotor (20°C). The pellet was suspended in 0·35 ml of 20 mM-Tris–HCl (pH 8·1), 5 mM-DTT, 5 mM-potassium glutamate, 0·20 mM-$CaCl_2$ and 1 mM-ATP. An equal volume of a solution containing 1·8 M-KCl, 50 mM-Tris–HCl (pH 8·7), 5 mM-potassium glutamate, 3 mM-$CaCl_2$, and 15 mM-ATP was then added. After swirling for 30 min at 0°C, the solution of depolymerized actin was spun for 5 min in a Beckman microfuge. The supernatant from this spin was layered onto a 1×25 cm Biorad P10 column previously equilibrated with G buffer (5 mM-Tris–HCl, pH 8·1, 0·2 mM-$CaCl_2$, 0·2 mM-ATP, and 0·2 mM-DTT). The protein pool in the void volume was adjusted to F buffer (50 mM-Tris–HCl, pH 8·1, 50 mM-KCl, 1 mM-ATP, 0·2 mM-$CaCl_2$, 0·2 mM-DTT) and left at room temperature for 45 min. Actin filaments were pelleted at 50 000 rev min^{-1} for 60 min at 4°C in a Beckman 50Ti rotor, resuspended in 300 μl of G buffer, and dialysed for 36 h at 4°C against G buffer to depolymerize actin filaments. The dialysed actin was then centrifuged for 7 min at 30 lbf in^{-1} in a Beckman airfuge. A final cycle of assembly and disassembly was carried out by adjusting the supernatant to F buffer, incubating at room temperature and repelleting the actin filaments. The pellet was resuspended in 150 μl of G buffer, dialysed for 36 h against G buffer containing 0·1 mM-DTT, centrifuged for 7 min at 30 lbf in^{-1} in a Beckman airfuge at 4°C and frozen on liquid nitrogen in small aliquots. The final protein yield was approximately 50 % and the stoichiometry was about 0·9 rhodamine molecules per actin monomer.

For both actin and tubulin, the stoichiometry of dye labelling did not change from one cycle of assembly to another, indicating that labelled and unlabelled proteins assemble with about equal efficiency. To estimate the stoichiometry of dye coupling, the concentration of dye linked to protein was determined by reading absorbance at 555 nm in 6 M-guanidinium–HCl (NHSR), or 0·1 M-Tris–HCl pH 9·5 (DTAF), with an extinction coefficient of 10^5 used for both tetramethyl rhodamine and fluorescein (see Kodak laboratory chemicals catalogue). Protein concentration was estimated by the Bradford procedure, using bovine serum albumin as a standard.

Embryo injections

Embryos were manually dechorionated and injected at 50 % egg length according to standard procedures (Santamaria, 1986). All solutions were spun for several minutes in a microfuge before loading into needles. The injected actin and tubulin tended to diffuse throughout the entire embryo within 10 min, although the concentration of the injected protein remained highest near the site of injection. In order to obtain solutions containing a mixture of NHSR–actin and DTAF–tubulin (Figs 4, 5) or NHSR–actin and NHSR–tubulin (Fig. 6), the appropriate protein solutions were mixed just before injection from the following stocks: 14 mg ml^{-1} DTAF–tubulin (stoichiometry = 0·45), 5·8 mg ml^{-1} NHSR–tubulin (stoichiometry = 0·6) and 5·6 mg ml^{-1} NHSR–actin (stoichiometry = 1·3).

Image recording

Injected embryos were photographed using a Nikon Diaphot-inverted microscope fitted with a 35 mm camera back. All micrographs were taken with a Zeiss ×100 neofluor objective; and a mercury arc lamp (HBO 100W) was used for illumination. Kodak Technical Pan 2415 film was hypersensitized by exposure to 4 lbf in^{-1} hydrogen at 30°C for 5 days (apparatus and information available from Lumicon, 2111 Research Drive, Livermore, CA 94550). This produces an ASA of approximately 1400 and allows a 2–4 s exposure, which greatly reduces photobleaching and blurring of the image due to cytoplasmic movements within the embryo. Video recordings were made using a Zeiss IM35 microscope and a Zeiss ×100 neofluor objective. A Zeiss halogen illuminator turned to full power was used as a light source for low-light-level video recordings, although satisfactory images could be obtained with lower light levels. The microscope was coupled to a Cohu SIT Camera and an image processor from Interactive Video Systems.

Fixation procedures

We have used two procedures for fixation of embryos for immunofluorescence. One is a slight modification of the procedure of Warn & Warn (1986). Dechorionated embryos are immersed in a mixture of 1 part heptane and 1 part 97 % methanol:3 % 0·5 M-Na_3EGTA (EGTA stock adjusted to pH 7·5) at room temperature. After shaking vigorously for 1 min, embryos that have lost their vitelline layer sink to the bottom of the tube. These are recovered and stored in the methanol/EGTA mixture for several hours at room temperature, or overnight at 4°C. The embryos are rehydrated by passage through a series of 20, 40, 60 and 80 % PBS in methanol. The fixation procedure of Karr & Alberts (1986) was carried out as described, except that twice as much formaldehyde was added.

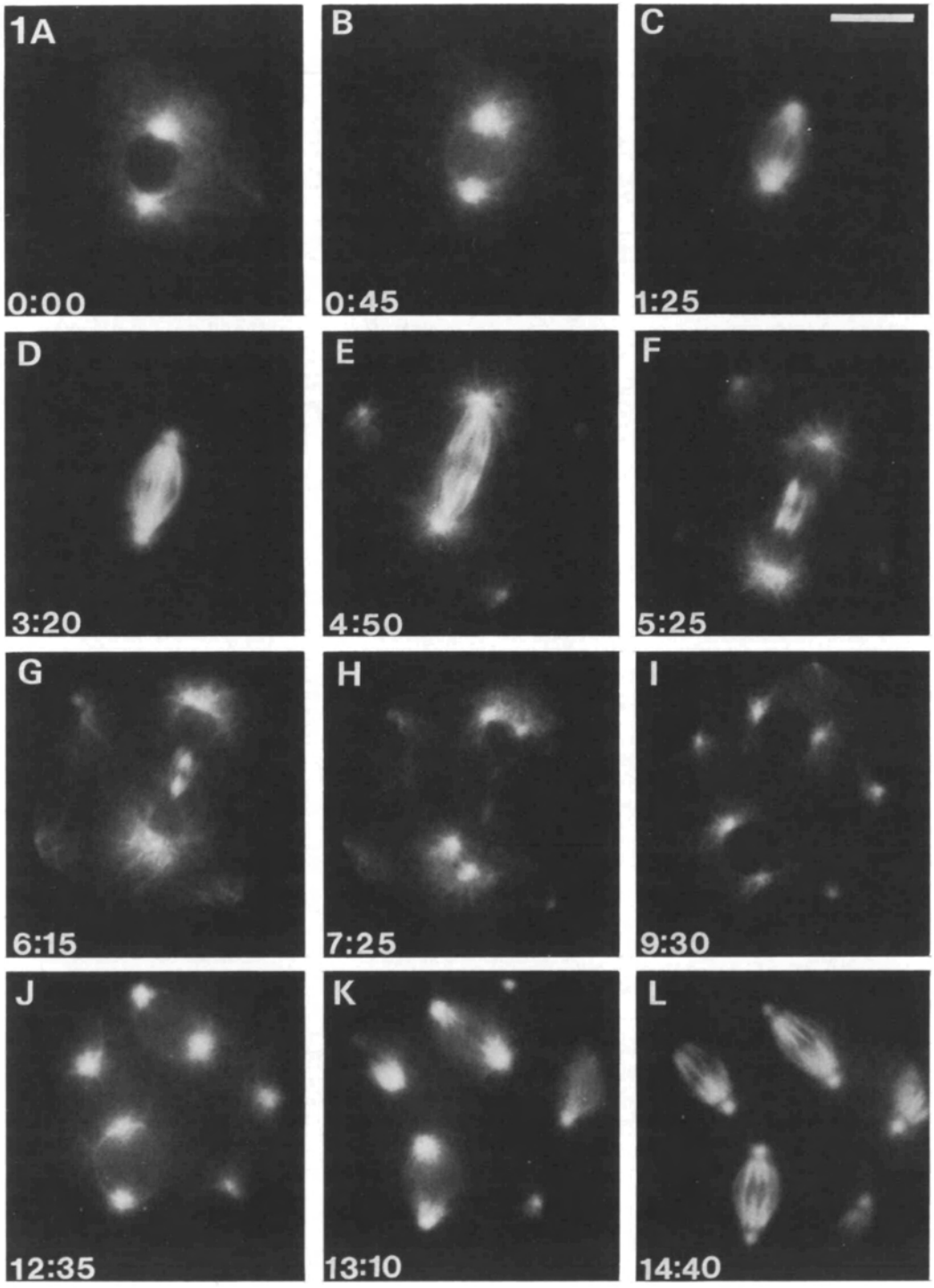

Fig. 1. The changes in microtubule distribution between interphase of nuclear cycle 10 and metaphase of nuclear cycle 11, as seen *in vivo* after microinjection of fluorescently labelled bovine tubulin. The embryo was injected 4 min prior to the first image shown with a 7 mg ml^{-1} solution of NHSR–tubulin (stoichiometry of 0·85 rhodamines per tubulin dimer) and images were recorded at the indicated time intervals with hypersensitized 35 mm film. All images were recorded from the same nucleus, with the microscope stage moved occasionally to prevent cytoplasmic contractions from moving the observed nucleus out of the field of view. The room temperature during the recording was 23°C. The nuclear cycle stages are as follows: (A) late interphase; (B) prophase; (C) prometaphase; (D) metaphase; (E) anaphase; (F) late anaphase; (G) telophase; (H) early interphase; (I) interphase; (J) prophase; (K) prometaphase; (L) metaphase. Bar, 10 μm.

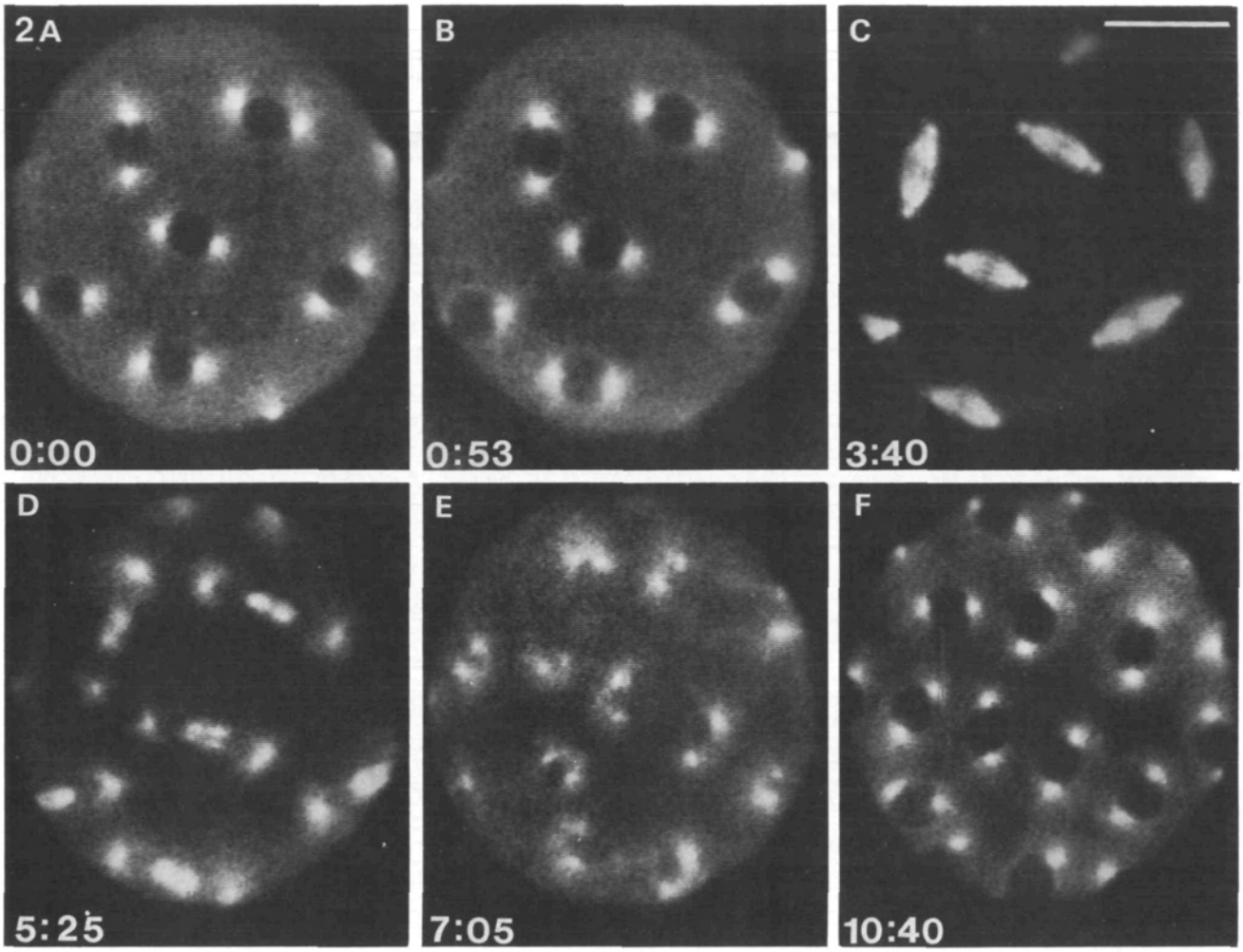

Fig. 2. The changes in microtubule distribution between interphase of nuclear cycle 10 and interphase of nuclear cycle 11, as visualized by low-light-level video techniques. The embryo was injected 6 min prior to the first image shown with a 7 mg ml^{-1} solution of NHSR bovine tubulin (stoichiometry of 0·85 rhodamines per tubulin dimer). Before beginning the recording, the image was moved out of focus and an averaged background image was obtained and stored in a frame buffer. The averaged background image was then digitally subtracted from a 16-frame running average of the live image. The room temperature during the recording was 22°C. The nuclear cycle stages are as follows: (A) late interphase; (B) prophase; (C) metaphase; (D) late anaphase; (E) early interphase; (F) interphase. Bar, 20 μm.

Results and Discussion

Fluorescent labelling of tubulin

We have used three fluorescent probes to label bovine tubulin: dichlorotriazinyl amino fluorescein (DTAF), lissamine rhodamine B sulphonyl chloride (LRSC), and *N*-hydroxy succinimidyl tetramethyl rhodamine (NHSR). For all three tubulins, reaction conditions yielding a labelling stoichiometry of 0·4–1·0 were selected, so that most of the labelled molecules carry only a single fluorescein (DTAF–tubulin) or rhodamine (LRSC–tubulin and NHSR–tubulin).

DTAF–tubulin is a well-characterized derivative that has been used in many other laboratories; it appears to function normally *in vitro* and *in vivo*, as shown by a variety of criteria (Keith *et al.* 1981; Leslie *et al.* 1984; and Salmon *et al.* 1984). However, the fluorescein chromophore is relatively light sensitive and is thus rapidly photobleached at the light levels needed for observation. To avoid this problem, we have preferred to use rhodamine reagents to label tubulin. As expected, tubulin labelled with LRSC is significantly more resistant to photobleaching. When LRSC–tubulin is injected into early *Drosophila* embryos or tissue culture cells, it becomes rapidly incorporated into endogenous microtubule networks. However, this incorporation is short-lived; within 5 min one observes a decrease in the labelling of tubulin networks, accompanied by the appearance of rhodamine fluorescence in vacuole-like structures (data not shown). This phenomenon occurs even in the dark and is presumably due to the selective

Table 1. *Timing of microtubule rearrangements*

(A) *Overview of mitosis of nuclear cycle 10 and interphase of nuclear cycle 11 (our data and Foe & Alberts, 1983)*

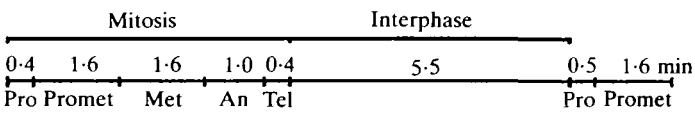

(B) *Data from injected embryos*

	Stage	Duration (s)
End of nuclear cycle 10	Prometaphase[a]	97 ± 6 (n = 3)
	Metaphase[b]	100 ± 8 (n = 3)
	Anaphase[c]	66 ± 12 (n = 7)
Start of nuclear cycle 11	Centrosome migration[d]	168 ± 16 (n = 8)
	Mid interphase and prophase[e]	223 ± 20 (n = 8)
	Prometaphase	91 ± 7 (n = 6)

The temperature during all recordings was 22–24°C. By convention, each nuclear cycle begins at the start of interphase.

[a] Nuclear envelope breakdown to completion of the mitotic spindle.

[b] Spindle completion to the beginning of spindle elongation.

[c] Beginning of spindle elongation to maximum spindle elongation.

[d] Maximum spindle elongation to completion of centrosomal migration; the period includes about 30 s of telophase (see table 2 of Foe & Alberts, 1983), but is mostly early to mid interphase.

[e] Completion of centrosomal migration to nuclear envelope breakdown; this period includes about 30 s of prophase (see table 2 of Foe & Alberts), but is mostly mid to late interphase.

proteolytic degradation of LRSC–tubulin.

Because the DTAF–tubulin is stable in the dark after its microinjection, the instability of the LRSC–tubulin is presumably due either to the rhodamine chromophore or to the different linkage of this chromophore to tubulin. Another rhodamine derivative was therefore prepared and tested by microinjection. Tubulin labelled with NHSR is both resistant to photobleaching and stable *in vivo*. When injected into embryos, the NHSR–tubulin is incorporated into endogenous microtubule networks in less than 30 s, and it provides strikingly clear images of microtubule arrays in the living embryo.

Microtubule networks in living embryos

The major *Drosophila* embryo tubulins are 96 % (alpha$_1$ tubulin) and 95 % (beta$_1$ tubulin) identical to their vertebrate analogues in porcine brain and chicken brain, respectively (Theurkauf *et al.* 1986; Rudolph *et al.* 1987). As a check on the suitability of bovine tubulin as a marker for *Drosophila* microtubules, tubulin was prepared from *Drosophila* embryos and labelled with LRSC (see Methods). When this tubulin was injected into embryos, it produced labelling patterns that were indistinguishable from those obtained with bovine tubulin (data not shown). Most experiments were therefore performed with bovine tubulin because of its ready availability from brain. We also saw no differences in the labelling patterns generated by the different fluorescent derivatives of tubulin; indicating that our tubulin derivatives are reliable *in vivo* probes.

Fig. 1 presents a series of fluorescence micrographs taken at the indicated time intervals of an embryo injected with a 7 mg ml^{-1} solution of NHSR–tubulin. We estimate that this amount of injected tubulin represents 2–5 % of the total tubulin pool in the *Drosophila* embryo, assuming that tubulin represents 3 % of the total protein (Loyd *et al.* 1981) and that the injected volume and the embryo volume are approximately 2×10^{-4} μl and $1{\cdot}5\times10^{-2}$ μl, respectively (Foe & Alberts, 1983). In order to reduce the background due to out-of-focus fluorescence and light scattering in these thick specimens, a ×100 times objective was used and the field diaphragm was closed down to include only a single nucleus. The nucleus shown in Fig. 1A is in late interphase; microtubules are seen to radiate from asters on either side of a dark region that corresponds to the nucleus. Fig 1B–L are identical views that show the changes in microtubule distribution that take place as this nucleus proceeds from interphase of cycle 10 through metaphase of cycle 11 in the syncytial blastoderm embryo. In cycle 10, the *Drosophila* embryo contains about 300 nuclei that are regularly arranged in a monolayer just beneath the egg plasma membrane (Zalokar & Erk, 1976; Foe & Alberts, 1983). All of these nuclei behave indistinguishably when viewed in this way (see also Karr & Alberts, 1986).

Video intensification techniques allow substantially lower light levels than the film procedures used for Fig. 1, and they thereby allow the continuous recording of embryos injected with fluorescently labelled proteins (for reviews see Bright & Taylor, 1986 and Inoue, 1986). Fig. 2 presents a series of photographs taken from a video monitor showing the changes in microtubule distribution that take place during the transition from nuclear cycle 10 to 11. Similar recordings have allowed single embryos to be monitored from cycles 10 through 14, a period of 2 h, without damage to the embryo – as judged by its subsequent hatching to a normal larva (data not shown).

Data such as those shown in Figs 1 and 2 reveal a regular pattern of changes in microtubule distribution during each nuclear cycle. Data for the timing of events in cycles 10 and 11 are compiled in Table 1. In telophase, a pair of centrosomes is located near the surface of the nucleus that is closest to the plasma membrane (Figs 1H and 2E). These centrosomes

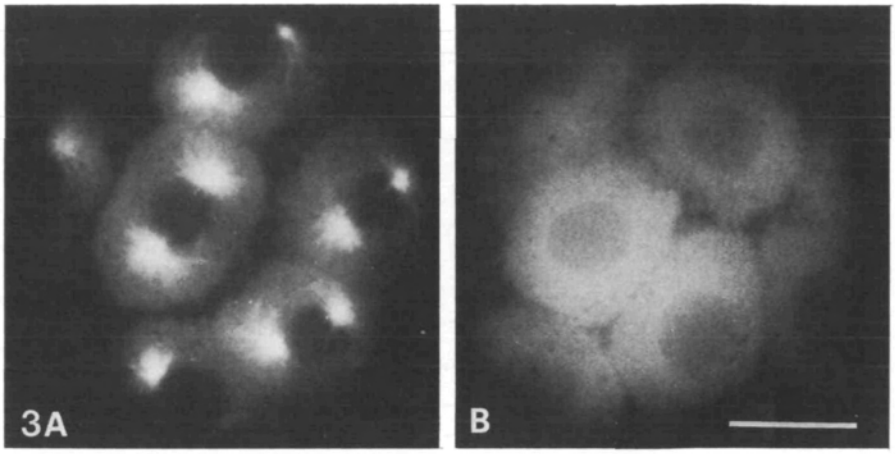

Fig. 3. The appearance of distinct domains surrounding each of the nuclei in the syncytial blastoderm. The embryo in Fig. 3A was injected with rhodamine-labelled bovine tubulin as in Figs 1 and 2. The embryo in Fig. 3B was injected with a rhodamine-labelled dextran of 35 000 M_r (a gift of Dr Jon Minden). Equivalent concentrations of rhodamine were injected in each case. Both embryos were in interphase of nuclear cycle 11 and the micrographs were taken from a focal plane just above the centre of the nucleus. Bar, 10 μm.

require a few minutes of interphase to migrate to opposite sides of the nuclear envelope, where they remain for a few more minutes before the next mitosis begins.

Throughout this interphase period, prominent astral microtubules emanate from each centrosome and extend away from the nucleus (Fig. 1A,I). After centrosome migration, some microtubules traverse the surface of the nucleus between the two centrosomes (not shown) and a fine ring of fluorescence appears that surrounds the nuclear envelope as mitosis begins (Figs 1J,B and 2B). A partial nuclear envelope breakdown follows (see Stafstrom & Staehlin, 1984), allowing the metaphase spindle to be assembled. This spindle has an unusual morphology, inasmuch as the poles appear to be separated by a small gap from the remainder of the spindle (Figs 1D,L and 2C); a similar morphology has been observed by electron microscopy in isolated spindles of the sea urchin embryo (Salmon & Segall, 1980). During metaphase, the spindles of adjacent nuclei often make short oscillatory movements relative to each other, typically making excursions of 3 μm or so. Early anaphase is marked by the appearance of prominent astral microtubules and the elongation of the spindle (Fig. 1E). The asters grow rapidly and by late anaphase the spindle is largely disassembled, leaving only a bundle of interzonal microtubules and large asters associated with each of the reforming daughter nuclei (Figs 1F and 2D). The interzonal microtubules persist well into telophase (Fig. 1G). Telophase ends with the paired centrosomes at their interphase position on top of each nucleus and the disappearance of the interzonal microtubules (Fig. 1H).

In addition to filamentous fluorescence, each nucleus is surrounded by a domain of weaker, diffuse fluorescence that persists throughout the nuclear cycle and is assumed to represent unpolymerized tubulin. This diffuse domain of fluorescence becomes clearest in interphase/prophase of nuclear cycle 11 (Fig. 3A). Similar domains of diffuse fluorescence are seen to surround each nucleus in embryos that have been injected with fluorescently labelled dextrans of 35 000 M_r (Fig. 3B). When focusing up and down through each nuclear domain, the separation between the adjacent domains in Fig. 3 is detected only in the half of each domain closest to the plasma membrane. It is therefore possible that the surface protrusions seen as 'somatic buds' above interphase and prophase nuclei by Foe & Alberts (1983) and Stafstrom & Staehlin (1984) produce the apparent separation in the fluorescent domains around each nucleus.

The viability of embryos is unaffected by injection of fluorescently labelled tubulin. Typically, 80–90 % of embryos injected with control buffer or labelled tubulin develop into normal hatching larvae. The amount of light required to visualize the labelled tubulin also does not seem to affect viability, since the majority of the embryos photographed develop into normal hatching larvae.

Our images of microtubule networks *in vivo* are consistent with those of Warn *et al.* (1987), who have used microinjection of a fluorescently labelled antibody against tyrosinated α-tubulin to visualize microtubule networks in living *Drosophila* embryos.

Fluorescent labelling of actin

We have used rabbit muscle actin labelled with

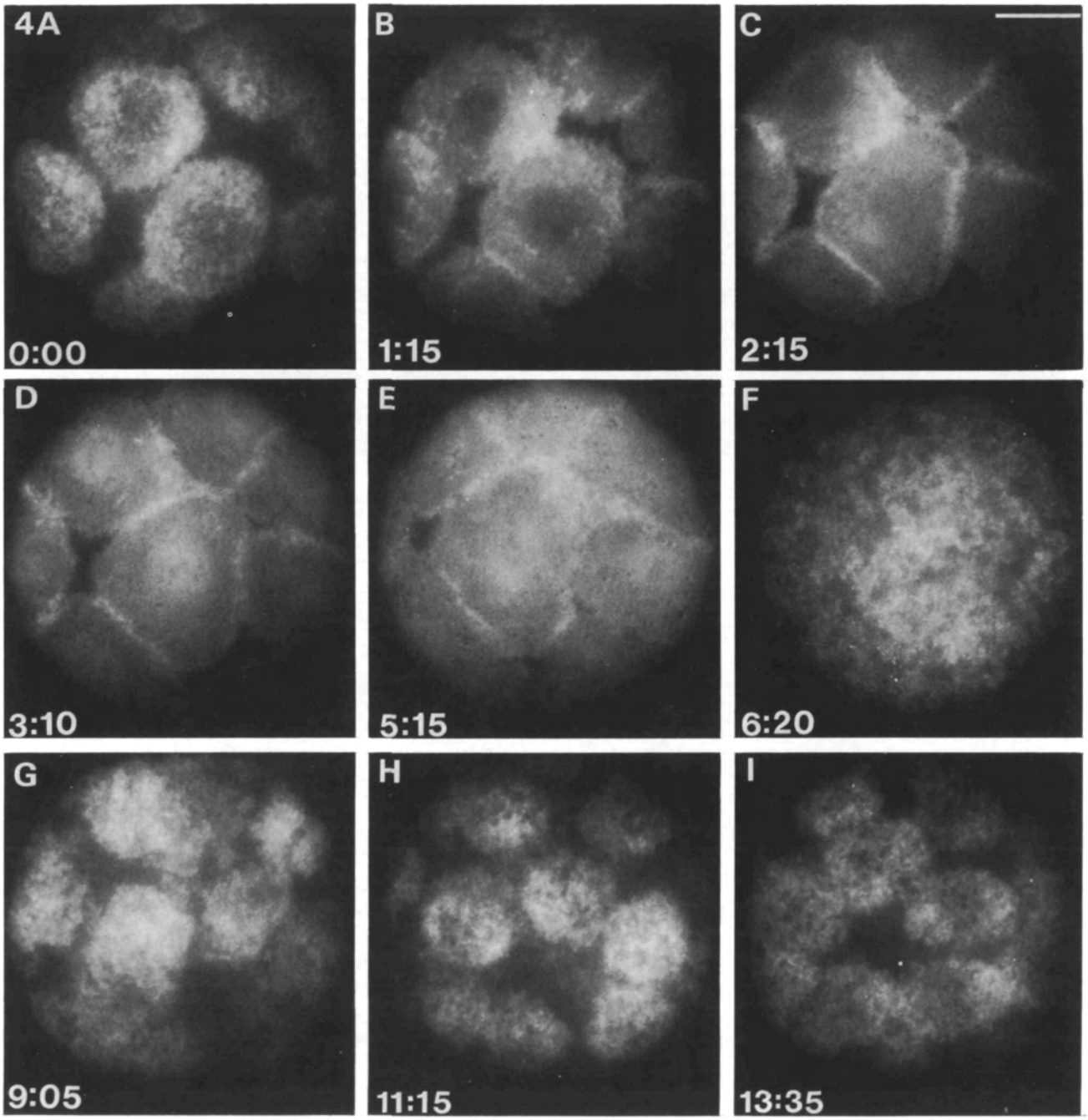

Fig. 4. The changes in actin distribution between interphase of nuclear cycle 11 and prophase of nuclear cycle 12, as visualized *in vivo* after microinjection of fluorescently labelled rabbit muscle actin. The embryo was injected 13 min prior to the first image shown with a solution of 4·5 mg ml^{-1} NHSR rabbit muscle actin (stoichiometry of 0·85 rhodamine molecules per actin monomer) and 5·0 mg ml^{-1} DTAF bovine tubulin (stoichiometry of 0·45 fluorescein molecules per tubulin dimer). Images were then recorded on hypersensitized 35 mm film at the indicated times. The photographs of the actin, taken with a rhodamine filter cassette, are presented here. The micrograph shown in A was taken from a focal plane at the surface of the actin caps overlying each of the nuclei. The micrographs in B–E were taken from a slightly deeper focal plane in order to show the development of the actin belts surrounding each of the nuclei at metaphase. The remaining micrographs (F–I) were taken from a surface focal plane. Each image is of the same group of nuclei, although the microscope stage had to be moved occasionally to prevent cytoplasmic contractions from moving the recorded region out of the field of view. The room temperature during the recordings was 22°C. The nuclear cycle stages were determined by intermittent inspection of the tubulin with a fluorescein filter cassette, as shown in Fig. 5; these stages were as follows: (A) interphase; (B) prophase; (C) prometaphase; (D) metaphase; (E) late metaphase; (F) anaphase; (G) telophase; (H) interphase; (I) early prophase. Note that nuclear cycle 11 is slightly longer than nuclear cycle 10 (Foe & Alberts, 1983). Bar, 10 μm.

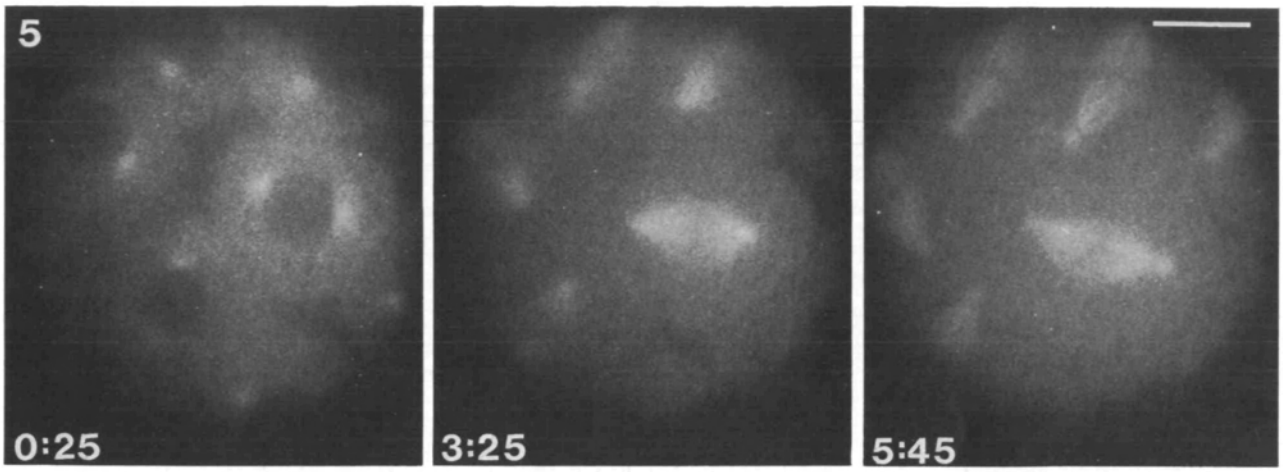

Fig. 5. The distribution of tubulin in the same group of nuclei recorded in Fig. 4, as visualized by DTAF–tubulin fluorescence. The embryo was injected with a mixture of NHSR–actin and DTAF–tubulin, as described in the legend to Fig. 4. Images of the DTAF–tubulin were obtained at the indicated times by replacing the rhodamine filter cassette with a fluorescein filter cassette. Bar, 10 μm.

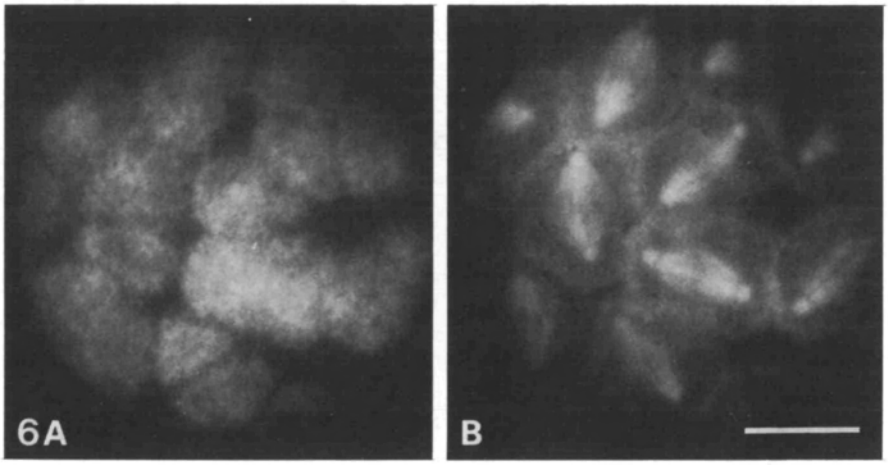

Fig. 6. The relative distributions of actin and tubulin at metaphase of nuclear cycle 12. An embryo was injected with a solution of 3·7 mg ml^{-1} NHSR–actin (stoichiometry of 1·3 rhodamines per actin monomer) and 1·9 mg ml^{-1} NHSR–tubulin (stoichiometry of 0·6 rhodamines per tubulin dimer). The micrographs were recorded on hypersensitized 35 mm film several minutes later. (A) A surface view of an embryo, showing a focal plane corresponding to the surface of the actin cap. (B) The same region viewed at essentially the same time at a deeper focal plane that shows each spindle to be surrounded by a belt of actin. Bar, 10 μm.

NHSR as a probe for actin filament networks in the *Drosophila* embryo. In our initial experiments, we labelled rabbit muscle actin in a pH 7·6 buffer – a standard condition used for preparing actin (Pardee & Spudich, 1982). This labelled actin behaved in a manner indistinguishable from unlabelled actin through two cycles of *in vitro* assembly and disassembly, and it rapidly became incorporated into the endogenous actin networks when injected into embryos. However, as with LRSC–tubulin, the actin labelled in this way was degraded within 5–10 min, producing a vacuolar staining pattern. This was unexpected, since tubulin labelled with NHSR is not degraded *in vivo*. Because the NHSR–tubulin had been labelled at pH 6·8, we repeated the NHSR labelling of actin at a lower pH. As with the pH 7·6 labelling, the actin labelled to a good stoichiometry at pH 6·8 and behaved normally through two cycles of *in vitro* polymerization and depolymerization. However, this actin showed no significant degradation *in vivo*. The absorbance spectra of the different NHSR–actins suggest that different functional groups are labelled at pH 7·6 and pH 6·8. The absorbance spectrum of actin labelled at pH 6·8 shows a largely monophasic peak in the rhodamine region (E_{max} at 555 nm), while actin labelled at pH 7·6 shows a

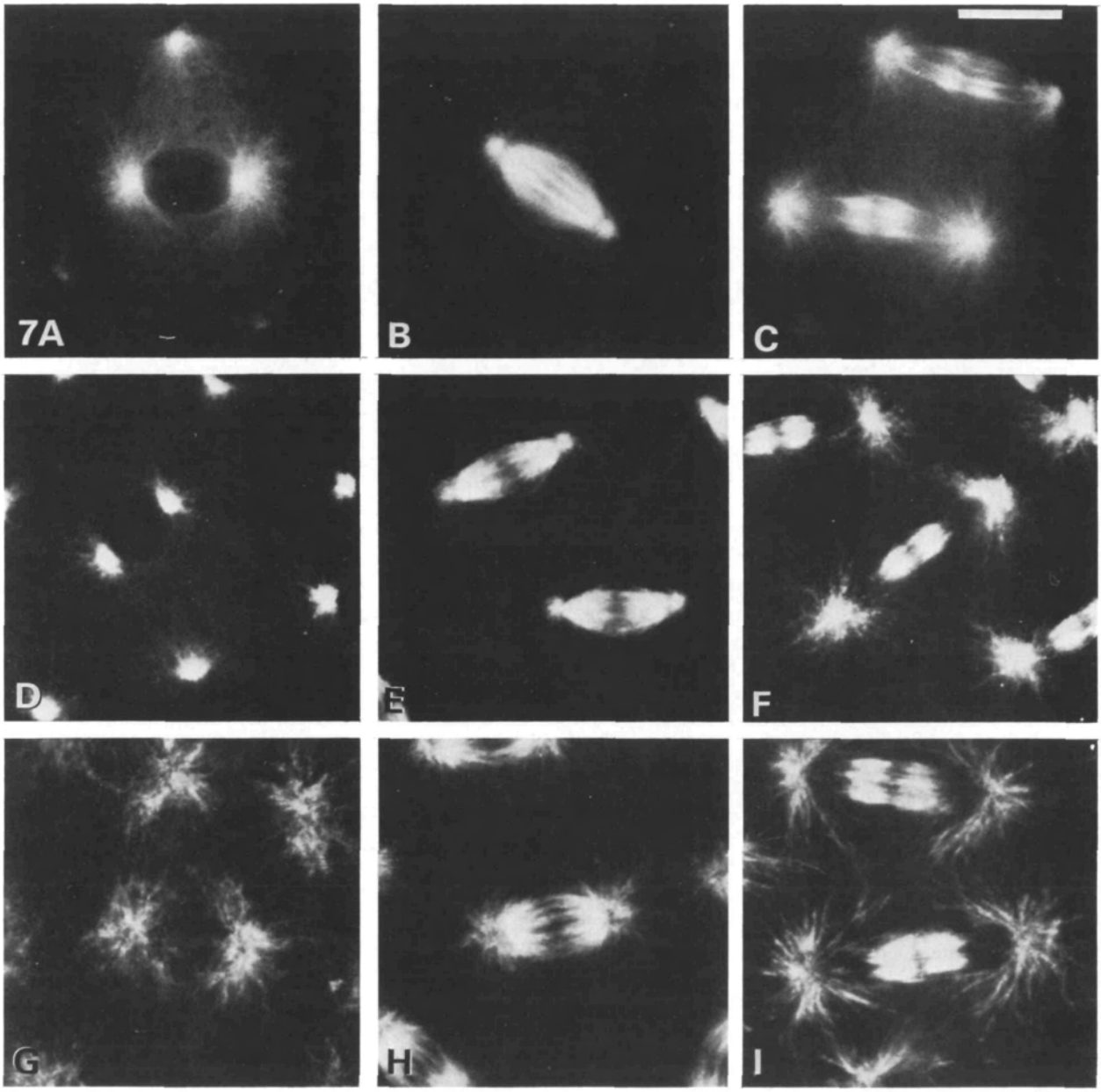

Fig. 7. A comparison of the distribution of the microtubules seen in living embryos with their distribution in whole fixed embryos. A–C show the distribution of microtubules observed *in vivo* after microinjection of fluorescently labelled bovine tubulin, in an experiment performed as described in the legend to Fig. 1. The three different stages of the nuclear cycle shown are: (A) prophase; (B) metaphase; (C) anaphase. D–F show the distribution of microtubules at approximately the same three stages in embryos that have been fixed with methanol (see text) and immunofluorescently stained for tubulin. Similarly, G–I show the distribution of microtubules at these stages in embryos fixed and stained by the Karr & Alberts (1986) procedure. Bar, 10 μm.

biphasic spectrum (peaks at 520 nm and 555 nm). We believe that the splitting of the rhodamine peak seen for actin labelled at pH 7·6 is due to an interaction of the rhodamine ring structure with the native actin molecule. This hypothesis is supported by the observation that the absorbance spectrum of the pH 7·6 NHSR–actin after denaturation with 6 M-guanidinium–HCl closely resembles the monophasic peak seen for the pH 6·8 labelled actin.

The actin filaments in living embryos

When the NHSR–actin prepared at pH 6·8 is injected into *Drosophila* embryos, it is incorporated into endogenous actin networks within less than a minute. As with fluorescently labelled tubulin, the viability of embryos is unaffected by injection of NHSR–actin. Fig. 4 presents a series of fluorescence micrographs showing the changes in actin distribution that take place from interphase of cycle 11 to prophase of

cycle 12. We were able to assign exact stages in the cell cycle by coinjecting fluorescein-labelled tubulin with the rhodamine-labelled actin. Fig. 5 presents several examples of fluorescence micrographs taken from the Fig. 4 embryo, with a switch to the fluorescein filter cassette used to visualize microtubules.

Our work with fluorescently labelled actin confirms the results of previous studies that used fixed embryos and a specific actin stain (Warn *et al.* 1984; Karr & Alberts, 1986). In interphase of nuclear cycle 11, each nucleus is centred beneath a flat cap-like layer of actin, which has a coarse fibrous appearance (Fig. 4A). As metaphase approaches, the cap enlarges by spreading laterally until it comes into contact with adjacent actin caps (Fig. 4B,C). In micrographs taken at a focal plane just below the surface actin layer, the actin at this stage can be seen to extend below the surface of the actin cap at the regions of contact between adjacent actin domains. By metaphase, each spindle is therefore surrounded by a shell of actin that extends over its surface and around its sides. This distribution of actin is particularly clear in embryos that have been coinjected with a mixture of NHSR–actin and NHSR–tubulin, so that both actin filaments and microtubules are labelled with rhodamine. Fig. 6 shows micrographs taken from such an embryo in metaphase of nuclear cycle 12. The micrograph at the left has been taken at a focal plane above the spindle and shows the surface of the actin cap (Fig. 6A); the other micrograph was taken at a deeper focal plane and shows the metaphase spindle surrounded by a belt of actin (Fig. 6B). During metaphase, a slight concentration of actin fluorescence can be seen in the region of the spindle (Fig. 4D,E). However, a similar concentration of fluorescence in the spindle region is seen in control embryos injected with equivalent amounts of fluorescently labelled dextran of 35 000 M_r (not shown). At anaphase, the actin domains elongate and the belts of actin surrounding each domain begin to disappear. By late anaphase or early telophase, the actin appears to form a continuous layer over the surface of the embryo (Fig. 4F), and it is difficult to detect evidence of individual domains corresponding to each nucleus. The actin domains reappear during late telophase (Fig. 4G), and by interphase each nucleus is again overlaid by its own unique actin cap just below the plasma membrane (Fig. 4H).

Tests of fixation procedures

The availability of the labelled embryos just described has allowed us to evaluate fixation procedures to determine which ones give immunofluorescent staining that most accurately mimics the images that we have obtained *in vivo*. By this criterion, microtubules were not perfectly preserved by any tested procedure, although the best results were obtained by using a variation of a methanol-fixation procedure (Warn & Warn, 1986). Fig. 7 compares the distribution of microtubules *in vivo* (Fig. 7A–C) and in methanol-fixed embryos (Fig. 7D–F) at three stages of the mitotic cycle. The figure shows that although the bulk distribution of microtubules is preserved in the methanol fixation, much of the fine structure is lost. Thus far we have been unable to find a better fixation procedure for microtubules. In particular, inclusion of glutaraldehyde in the methanol fixation procedure (0·1–1 %) did not seem to improve significantly the preservation of microtubules. The formaldehyde/taxol procedure used by Karr and Alberts gives striking images, but it causes an explosion of the centrosomal region and the appearance of excess astral microtubules during interphase and prophase (Fig. 7G–I).

Similar studies show that actin is reasonably well preserved by the methods of Warn *et al.* (1984) and Karr & Alberts (1986), and that the methanol fixation that best preserves microtubules poorly preserves actin networks (not shown).

We would like to acknowledge David M. States for his expert preparation of the manuscript. This research was supported by NIH grant no. GM23928 to B.S.A. and by NIH institutional training grant no. GM08120 to D.R.K.

References

BRIGHT, G. R. & TAYLOR, D. L. (1986). In *Applications of Fluorescence in the Biomedical Sciences* (ed. D. A. Taylor, A. S. Waggoner, R. F. Murphy, F. Lanni & R. R. Birge), pp. 257–288. New York: Alan R. Liss, Inc.

EDGAR, B. A., ODELL, G. M. & SCHUBIGER, G. (1988). Cytoarchitecture and the patterning of *fushi tarazu* expression in the Drosophila blastoderm. *Genes and Development* (In press).

DETRICH, H. W. & WILSON, L. (1983). Purification, Characterization, and Assembly Properties of Tubulin from Unfertilized Eggs of the Sea Urchin Strongylocentrotus purpuratus. *Biochemistry* **22**, 2453–2462.

FOE, V. E. & ALBERTS, B. M. (1983). Studies of nuclear and cytoplasmic behavior during the five mitotic cycles that precede gastrulation in Drosophila embryogenesis. *J. Cell Sci.* **61**, 31–70.

INOUE, S. (1986). *Video Microscopy*. New York: Plenum Press.

KARR, T. L. & ALBERTS, B. M. (1986). Organization of the cytoskeleton in early Drosophila embryos. *J. Cell Biol.* **102**, 1494–1509.

KEITH, C. H., FERAMISCO, J. R. & SHELANSKI, M. (1981). Direct visualization of fluorescein-labeled microtubules *in vitro* and in microinjected fibroblasts. *J. Cell Biol.* **88**, 234–240.

LESLIE, R. J., SEXTON, W. M., MITCHISON, T. J., NEIGHBORS, B., SALMON, E. D. & MCINTOSH, J. R. (1984). Assembly properties of fluorescein labeled tubulin before and after fluorescence photobleaching. *J. Cell Biol.* **99**, 2146–2156.

LOYD, J. E., RAFF, E. C. & RAFF, R. A. (1981). Site and timing of synthesis of tubulin and other proteins during oogenesis in *Drosophila melangaster. Devl Biol.* **86**, 272–284.

MITCHISON, T. J. & KIRSCHNER, M. W. (1984). Microtubule assembly nucleated by isolated centrosomes. *Nature, Lond.* **312**, 232–237.

PARDEE, J. D. & SPUDICH, J. A. (1982). Purification of muscle actin. *Methods Enzymol.* **85**, 164–181.

RABINOWITZ, M. (1941). Studies on the cytology and early embryology of the egg of *Drosophila melanogaster. J. Morph.* **69**, 1–49

RUDOLPH, J. E., KIMBLE, M., HOYLE, H. D., SUBLER, M. A. & RAFF, E. C. (1987). Three *Drosophila* beta-tubulin sequences; a developmentally regulated isoform (beta-3), the testis-specific isoform (beta-2), and an assembly-defective mutation of the testis-specific isoform (B2t8) reveal both an ancient divergence in metazoan isotypes and structural contraints for beta-tubulin function. *Molec. Cell Biol.* **7**, 2231–2242.

SALMON, E. D. & SEGALL, R. R. (1980). Calcium-labile mitotic spindles isolated from Sea Urchin eggs (*Lytechinus variegatus*). *J. Cell Biol.* **86**, 355–365.

SALMON, E. D., LESLIE, R. J., SAXTON, W. M., KAROW, M. & MCINTOSH, J. R. (1984). Spindle microtubule dynamics in sea urchin embryos. Analysis using fluorescence-labeled tubulin and measurements of fluorescence redistribution after laser photobleaching. *J. Cell Biol.* **99**, 2165–2174.

SANTAMARIA, P. (1986). Injecting Eggs. In *Drosophila: a Practical Approach* (ed. D. Roberts), pp. 159–174. Washington, DC: IRL Press.

SCRIBA, M. E. L. (1964). Beeinflussung der Fruhen Embryonalentwicklung von Drosophila melanogaster durch chromosomenaberrationen. *Zool. Jb. Anat. Bd.* **81**, 435–490.

SONNENBLICK, B. P. (1950). The early embryology of *Drosophila melanogaster.* In *Biology of Drosophila* (ed. M. Demerec), pp. 62–167. New York: John Wiley & Sons, Inc. Reprinted in 1965. New York and London: Hafner.

STAFSTRON, J. P. & STAEHLIN, L. A. (1984). Dynamics of the nuclear envelope and of nuclear pore complexes during mitosis in the *Drosophila* embryo. *Eur. J. Cell Biol.* **34**, 179–189.

STROME, S. & WOOD, W. B. (1983). Generation of asymmetry and segregation of germ-line specific granules in early *C. elegans* embryos. *Cell* **35**, 15–25.

TAYLOR, D. L., AMATO, P. A., MCNEIL, P. L., LUBY-PHELPS, K. & TANASUGARN, L. (1986). In *Applications of Fluorescence in the Biomedical Sciences* (ed. D. A. Taylor, A. S. Waggoner, R. F. Murphy, F. Lanni & R. R. Birge), pp. 347–376. New York: Alan R. Liss, Inc.

TAYLOR, D. L. & WANG, Y.-L. (1980). Fluorescently labeled molecules as probes of the structure and function of living cells. *Nature, Lond.* **284**, 405–410.

THEURKAUF, W. E., BRIUM, H., BO, J. & WENSINK, P. C. (1986). Tissue-specific and constitutive α-tubulin genes of *Drosophila melanogaster* code for structurally distinct proteins. *Proc. natn. Acad. Sci. U.S.A.* **83**, 8477–8481.

TURNER, R. R. & MAHOWALD, A. P. (1976). Scanning electron microscopy of *Drosophila* embryogenesis. I. The structure of the egg envelope and the formation of the cellular blastoderm. *Devl Biol.* **50**, 95–108.

UBBELS, G. A., HARA, K., KOSTER, C. H. & KIRSCHNER, M. W. (1983). Evidence for a functional role of the cytoskeleton in determination of the dorsoventral axis in *Xenopus laevis* eggs. *J. Embryol. exp. Morph.* **77**, 15–37.

WALTER, M. & ALBERTS, B. M. (1984). Intermediate filaments in tissue culture cells and early embryos of *Drosophila melanogaster.* In *Molecular Biology of Development, UCLA Symposium on Molecular and Cellular Biology, New Series* (ed. R. Firtel & E. Davidson), pp. 263–272. New York: Alan R. Liss, Inc.

WARN, R. M., FLEGG, L. & WARN, A. (1987). An investigation of microtubule organization and functions in living *Drosophila* embryos by injection of a fluorescently labeled antibody against tyrosinated α-tubulin. *J. Cell Biol.* **105**, 1721–1730.

WARN, R. M., MAGRATH, R. & WEBB, S. (1984). Distribution of F-actin during cleavage of the *Drosophila* syncytial blastoderm. *J. Cell Biol.* **98**, 156–162.

WARN, R. M., SMITH, L. & WARN, A. (1985). Three distinct distributions of F-actin occur during the divisions of polar surface caps to produce pole cells in *Drosophila* embryos. *J. Cell Biol.* **100**, 1010–1015.

WARN, R. M. & WARN, A. (1986). Microtubule arrays present during the syncytial and cellular blastoderm stages of the early *Drosophila* embryo. *Expl. Cell Res.* **163**, 201–210.

ZALOKAR, M. & ERK, I. (1976). Division and migration of nuclei during early embryogeneis of *Drosophila melanogaster. J. Microbiol. Cell.* **25**, 97–106.

(Accepted 20 April 1988)